Article

Not peer-reviewed version

# Anti-Cancer Outcome of Glucocorticoid Receptor Transrepression by Synephrine Derivatives

Ekaterina M. Zhidkova [†] , Ekaterina D. Savina [†] , Daria V. Migaleva , Olga A. Vlasova , Timur T. Valiev , Adel D. Enikeev , Gennadii A. Badun , Maria G. Chernysheva , Svetlana A. Dodonova , Alexey A. Kryukov , Pavel A. Kusov , Kirill V. Gordeev , Ekaterina A. Yurchenko , Andrey V. Matveev , Marianna G. Yakubovskaya , Ekaterina A. Lesovaya [*]

Posted Date: 24 October 2025

doi: 10.20944/preprints202510.1879.v1

Keywords: glucocorticoid; selective glucocorticoid receptor agonist/modulator; lymphoma; leukemia; transrepression; transactivation; osteoporosis; skin atrophy; primary lymphoblast; synephrine derivatives

*Article*

# Anti-Cancer Outcome of Glucocorticoid Receptor Transrepression by Synephrine Derivatives

**Ekaterina M. Zhidkova [1,†], Ekaterina D. Savina [1,†], Daria V. Migaleva [1], Olga A. Vlasova [1], Timur T. Valiev [2], Adel D. Enikeev [3], Gennadii A. Badun [4], Maria G. Chernysheva [4], Svetlana A. Dodonova [5], Alexey A. Kryukov [5], Pavel A. Kusov [1], Kirill V. Gordeev [6], Ekaterina A. Yurchenko [7], Andrey V. Matveev [8], Marianna G. Yakubovskaya [1,9] and Ekaterina A. Lesovaya [1,9,10,*]**

[1] Department of Chemical Carcinogenesis, Institute of Carcinogenesis, N.N. Blokhin National Medical Research Center of Oncology, Ministry of Health of Russia, Kashirskoe shosse 24-15, Moscow 115478, Russia
[2] Department of Hemoblastosis Chemotherapy, Institute of Pediatric Oncology and Hematology, N.N. Blokhin National Medical Research Center of Oncology, Ministry of Health of Russia, Kashirskoe shosse 24-15, Moscow 115478, Russia
[3] Oncogen Regulation Department, Institute of Carcinogenesis, N.N. Blokhin National Medical Research Center of Oncology, Ministry of Health of Russia, Kashirskoe shosse 24-15, Moscow 115478, Russia
[4] Department of Chemistry, M.V. Lomonosov Moscow State University, Leninskiye Gory 1, Moscow 119991, Russia
[5] Kursk State Medical University, Karl Marx St. 3, Kursk 305041, Russia
[6] Gamaleya Research Institute of Epidemiology and Microbiology, Gamalei St 18, Moscow 123098, Russia
[7] G.B. Elyakov Pacific Institute of Bioorganic Chemistry, 159 Prospect 100-Letiya Vladivostoka, Vladivostok 690022, Russia
[8] Department of Biotechnology and Industrial Pharmacy, Lomonosov Institute of Fine Chemical Technologies, MIREA - Russian Technological University, 86 Vernadsky Prospekt, Moscow 119571, Russia
[9] Institute of Medicine, Peoples' Friendship University of Russia, Miklukho-Maklaya St. 6, Moscow 117198, Russia
[10] Oncology Department, Ryazan State Medical University Named after Academician I.P. Pavlov, Ministry of Health of Russia, Ryazan 390026, Russia
* Correspondence: lesovenok@yandex.ru
† These authors contributed equally to this work.

## Abstract

**Background/Objectives**: Glucocorticoids (GCs) present effective anti-cancer drugs for the treatment of hematological malignancies but their clinical use is limited due to their multiple adverse effects. Selective glucocorticoid receptor agonists/modulators (SEGRAMs) modify glucocorticoid receptor (GR) function shifting it towards therapeutically important transrepression and, therefore, could be safer alternative to GCs. Here we report on biological activity of four novel ligands of glucocorticoid receptor (GR), derivatives of natural origin molecule, synephrine. **Methods**: We demonstrated the affinity of synephrine derivatives in silico and in vitro by molecular dynamics simulation and radioligand binding assay, correspondingly. Further, we tested the induction of apoptosis in cultured cells and cytotoxic effects in primary lymphoblasts from the patients with acute lymphoblastic leukemia. Therapeutically important GR transrepression was evaluated by luciferase reporter assay and Q-PCR of transrepression marker genes, while GR transactivation associated with side effects was evaluated by Q-PCR analysis and by the level of GR phosphorylation at Ser211. Anti-cancer effects of leader compound, 1-[4-(benzyloxy)phenyl]-2-(hexylamino)ethanol (10S-E2), was studied on murine transplantable lymphoma P388 model. 10S-E2 potential to avoid the development of atrophic complication was evaluated on the murine model of glucocorticoid-induced osteoporosis. **Results:** All studied synephrine derivatives demonstrated high GR affinity; the effects on GR function were

 doi:10.20944/preprints202510.1879.v1



controversial. The leader compound, 10S-E2 revealed SEGRAM properties in vitro and demonstrated anti-cancer effects in vivo. **Conclusion:** Although the anti-cancer effect of 10S-E2 was less pronounced to the reference drug dexamethasone, non-atrophogenic properties of 10S-E2 make this molecule an attractive candidate for long-term GR-associated therapies.

**Keywords:** glucocorticoid; selective glucocorticoid receptor agonist/modulator; lymphoma; leukemia; transrepression; transactivation; osteoporosis; skin atrophy; primary lymphoblast; synephrine derivatives

## 1. Introduction

Glucocorticoids (GCs) are an important class of immunosuppressive drugs used to treat various hematological malignancies and inflammatory diseases [1–3]. However, because GC are involved in gluconeogenesis signaling, cell proliferation and apoptosis, and bone formation, long-term treatment of patients with high-dose GCs is associated with various side effects, including hyperglycemia, type 2 diabetes mellitus, bone, muscle, and skin atrophy, and many other atrophic and metabolic complications [4–7].

Upon entering the cell, GCs bind to the glucocorticoid receptor (GR), a member of the nuclear receptor superfamily and a well-known transcription factor. Ligand binding induces conformational changes and dissociation of the GR multiprotein complex with chaperones. Phosphorylation of specific serine and tyrosine residues and nuclear translocation of GR results in the binding of glucocorticoid-responsive elements (GRE) or negative GRE in gene promoters, enhancers, or silencers, thereby stimulating or suppressing gene transcription (transactivation (TA) or transrepression (TR), respectively) [3,8,9]. Additionally, GR reveals non-genomic effects through protein-protein interactions with pro-proliferative and pro-inflammatory transcription factors (NF-kB, AP-1, STAT family proteins, etc.) following the attenuation of TF activity and DNA-independent TR [10–12]. Negative regulation by TR underpins the therapeutic effects while GR TA results in metabolic and atrophic complications, as well as GC resistance [10,12,13].

The development of selective glucocorticoid receptor agonists/modulators (SEGRAMs) aimed to reduce the side effects of GC treatment by separating GR TA and TR activities. Numerous steroidal and non-steroidal SEGRAMs have been described in the literature, including molecules of natural and synthetic origin, with potential applications in the treatment of inflammatory diseases and cancer [5,12,14–20].

Several SEGRAMs have entered clinical trials, but to date, no drug from the SEGRAM class has reached the market [21–29]. Further research is needed in the development of new molecules and expansion of the SEGRAM list, as well as in the clinical evaluation of beneficial and harmful effects.

Recently, we designed and synthesized synephrine derivatives as potential SEGRAMs. Preliminary screening of cytotoxic activity on leukemia and lymphoma cells demonstrated the highest affinity in silico of the most cytotoxic compound, 1-[4-(benzyloxy)phenyl]-2-(hexylamino)ethanol (10S-E2), as well as less toxic synephrine derivatives with the potential to bind GR: 2-(hexylamino)-1-(4-methoxyphenyl)ethanol (4S-C2), 1-(4-(benzyloxy)phenyl)-2-((2-hydroxyethyl)amino)ethanol (8S-E3) and 2-(hexylamino)-1-(4-nitrophenyl)ethanol (13S-G2) (Figure 1 and [30]).

 doi:10.20944/preprints202510.1879.v1



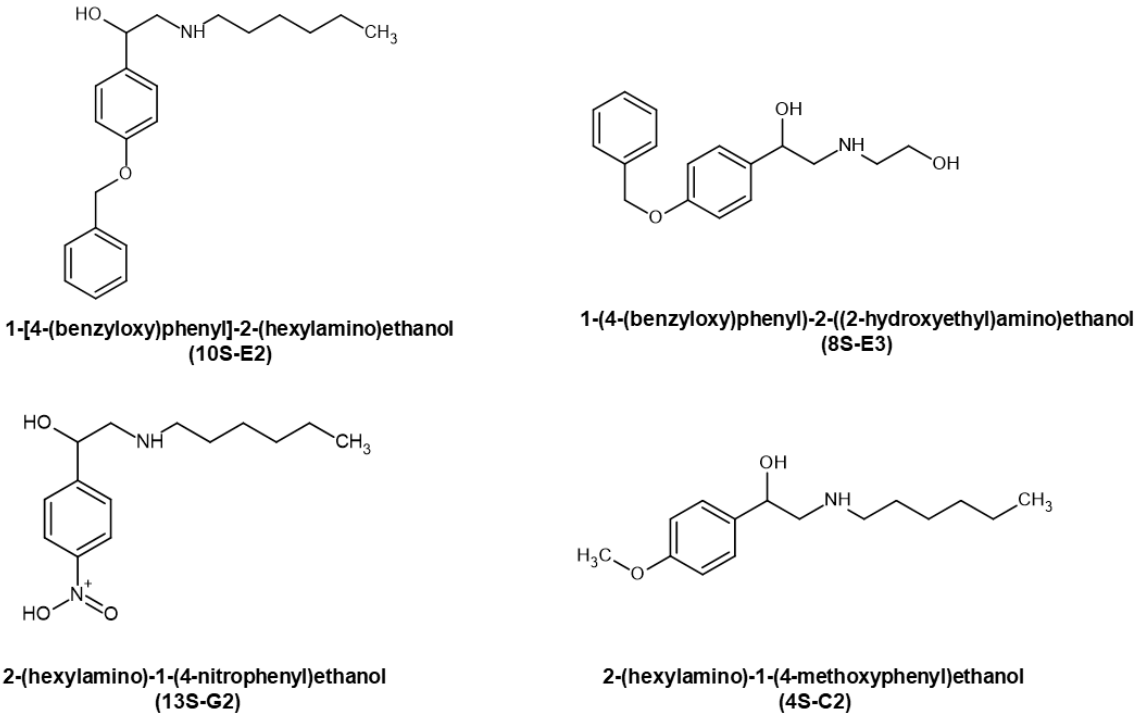


**Figure 1.** Structures of the synephrine derivatives 4S-C2, 8S-E3, 10S-E2 and 13S-G2.

Here, we report the molecular mechanisms underlying the in vitro effects of synephrine derivatives and the in vivo moderate anti-cancer activity of the most active compound, 10S-E2. Moreover, we assessed the atrophogenic effect of 10S-E2 in comparison with the glucocorticoid dexamethasone in osteoporosis and skin atrophy murine models and demonstrated the absence of atrophogenic potential of the novel synephrine derivative, as opposed to dexamethasone.

## 2. Results

### *2.1. Evaluation of Affinity of Synephrine Derivatives to GR*

The affinities of 4S-C2, 8S-E3, 10S-E2, and 13S-G2 for GR were proposed by molecular docking [30]. Here, we aimed to analyze the short-term stability of the complexes of tested compounds with GR by molecular dynamics simulation *in silico*, as well as to evaluate the binding of 4S-C2, 8S-E3, 10S-E2, and 13S-G2 to GR using a radioligand binding assay *in vitro*.

For the molecular dynamics study, the structures of the stereoisomers of 4S-C2, 8S-E3, 10S-E2, and 13S-G2 at the C-7 position were obtained and minimized (Supplementary Figure 1). Blind molecular docking to GR (PDB ID 1P93) was performed to identify the most favorable complexes of compounds with LBD-GR (Supplementary Table S2, Supplementary Figure S2). The 4S-C2 stereoisomers were predicted not to interact with key Arg611, Gln642, and Thr739 residues in LBD-GR, whereas 8S-E3, 10S-E2, and 13S-G2 may interact with Arg611, Gln642, or Thr739 (Supplementary Table S2, Supplementary Figure S2). Molecular dynamics simulations for 4 ns demonstrated that all ligand-GR complexes were stable (Table 1). The change in the Root Mean Square Deviation (RMSD) of the protein conformation was estimated to be no more than 1.140 Å. Stereoisomers 4S-C2_7$\alpha$ and 4S-C2_7$\beta$ exhibited the most unstable interactions with GR. For stereoisomers 8S-E3, 10S-E2, and 13S-G2, periodic changes were also observed in the ligand conformations, including those associated with the loss or formation of hydrogen bonds in the complex (Table 1, Supplementary Figures S3–S10). The most promising compound, 10S-E2 [30], was also tested in a 10 ns simulation and was demonstrated to form a stable complex throughout the 10 ns trajectory (Table 1, Figure 2A,B, Supplementary Figures S11–S12).

 doi:10.20944/preprints202510.1879.v1



**Table 1.** RSMD data of complexes of synephrine derivatives with GR.

| Time of simulation | Compound | | | | | | | | |
|---|---|---|---|---|---|---|---|---|---|
| **4 ns** | | **protein** | | | | **ligand** | | | |
| | | **avr** | **sd** | **min** | **max** | **avr** | **sd** | **min** | **max** |
| | 4S-C2_7α | 1.043 | 0.048 | 0.399 | 1.128 | 0.822 | 0.125 | 0.138 | 1.194 |
| | 4S-C2_7β | 1.048 | 0.049 | 0.395 | 1.134 | 0.883 | 0.100 | 0.228 | 1.139 |
| | 8S-E3_7α | 1.055 | 0.055 | 0.388 | 1.150 | 0.474 | 0.067 | 0.09 | 0.678 |
| | 8S-E3_7β | 1.042 | 0.044 | 0.4 | 1.112 | 0.488 | 0.094 | 0.139 | 0.860 |
| | 10S-E2_7α | 1.042 | 0.042 | 0.387 | 1.106 | 0,565 | 0,117 | 0,120 | 0,999 |
| | 10S-E2_7β | 1.057 | 0.073 | 0.007 | 1.140 | 0.497 | 0.079 | 0.095 | 0.769 |
| | 13S-G2_7α | 1.062 | 0.049 | 0.392 | 1.136 | 0.550 | 0.122 | 0.140 | 0.886 |
| | 13S_G2_7β | 1.060 | 0.042 | 0.378 | 1.120 | 0.561 | 0.118 | 0.168 | 0.932 |
| **10 ns** | | **protein** | | | | **ligand** | | | |
| | | **avr** | **sd** | **min** | **max** | **avr** | **sd** | **min** | **max** |
| | 10S-E2_7α | 1.070 | 0.041 | 0.387 | 1.157 | 0.319 | 0.081 | 0.110 | 0.707 |
| | 10S-E2_7β | 1.089 | 0.041 | 0.397 | 1.175 | 0.550 | 0.118 | 0.100 | 0.939 |

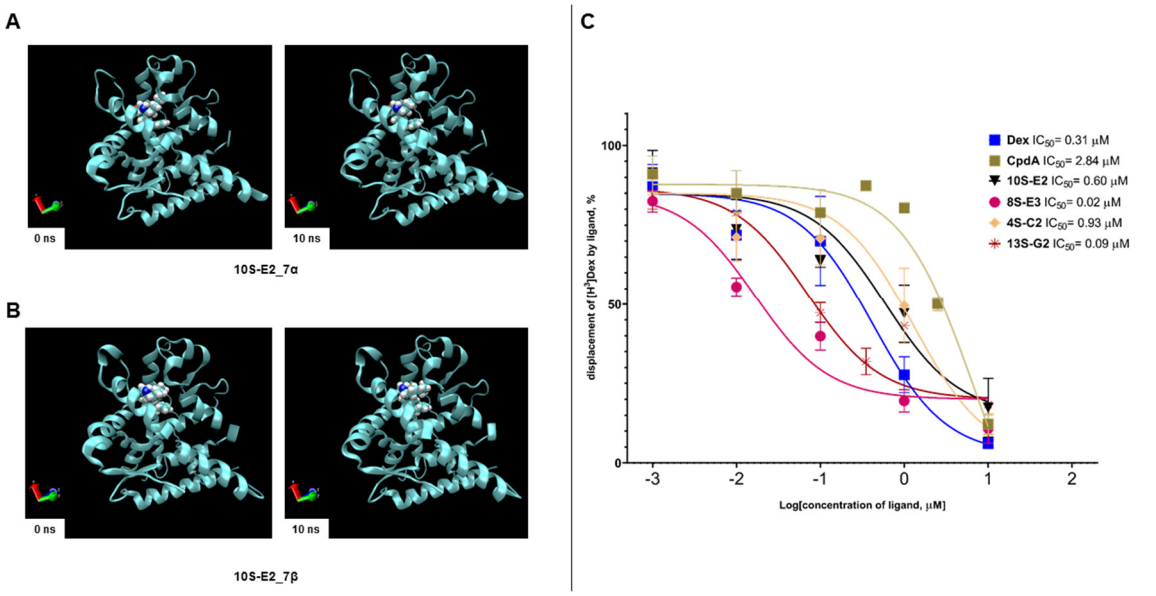


**Figure 2.** Evaluation of 4S-C2, 8S-E3, 10S-E2, 13S-G2 affinity to GR. **A, B**. Molecular dynamics simulation of the GR complex with 10S-E2_7α (A) and 10S-E2_7β (**B**) at the beginning of the trajectory and 10 ns later. The stability of the complex was simulated using molecular dynamics in the GROMACS program. **C**. GR binding affinity was estimated using a radioligand binding assay. Dex, 4S-C2, 8S-E3, 10S-E2, and 13S-G2 at various concentrations were added to each reaction tube and incubated for 90 min. Cell lysate radioactivity was measured using a RackBeta 1215 LC (LKB Wallac, Turku, Finland) spectrometer for 4 min. The results are presented as the percentage of the individual signal from [3H]Dex.

In vitro, the synephrine derivative compounds were tested in the concentration range of 0.001–10 μM. We demonstrated that the binding $IC_{50}$ values for the reference GR ligands Dex and CpdA were 0.31 μM and 2.84 μM, respectively, which is in accordance with the literature data, including our previous study [14,37–39]. $IC_{50}$ values of 4S-C2, 8S-E3, 10S-E2, and 13S-G2 varied from micromolar to nanomolar range: 4S-C2 – 3.21 μM, 8S-E3 – 0.08 μM, 10S-E2 – 0.56 μM, 13S-G2 – 0.69 μM (Figure 2C). The obtained data indicated that 8S-E3 had the highest affinity in the studied group, and the affinities of 10S-E2 and 13S-G2 were comparable to that of Dex. It should be considered that 10S-E2 and 13S-G2 were the most cytotoxic synephrine derivatives, with cell viability $IC_{50}$ values in

 doi:10.20944/preprints202510.1879.v1



the range of 13-26 μM in leukemia and lymphoma cells, while the $IC_{50}$ of 8S-E3 cytotoxic action was in the range of 80-120 μM [30]. Therefore, 10S-E2, 13S-G2, and 8S-E3 are the most promising GR ligands with anti-cancer effects.

### *2.2. Effects of Synephrine Derivatives on GR Functions*

To assess the effect of synephrine derivatives 4S-C2, 8S-E3, 10S-E2, and 13S-G2 on GR TA function, we performed Q-PCR analysis of the expression of known GR-target genes, including FKBP51, GILZ, and DDIT4 [19,32,33,40–42], after incubation for 4 h for FKBP51 and GILZ genes and 24 h for DDIT4 gene with the compounds under study or Dex as a reference drug. Depending on the treatment duration and cell line, Dex induced a 5-30-fold increase in the expression of TA marker genes, whereas compounds 10S-E2 and 13S-G2 did not increase the expression of the abovementioned genes (Figure 3A). The effects of 4S-C2 and 8S-E3 were controversial: 8S-E3 strongly attenuated DDIT4 expression by more than three times in K562 cells but induce a 1,5-fold decrease in this gene expression in Granta cells. These results require further investigation and adjustment of the experimental framework (Figure 3A). Q-PCR results were confirmed by Western blot analysis of the level of GR phosphorylated by Ser211 known as crucial protein modification for GR TA realization [43]. Treatment of the cells with Dex as a comparator and compounds 4S-C2, 8S-E3, and 13S-G2 induced a weak increase in GR phosphorylation level, whereas 10S-E2 did not affect the phosphorylation of GR by Ser211, which was in accordance with Q-PCR data (Figure 3B).

We analyzed GR TR function using NF-kB.Luc reporter assay with the irritating inflammatory agent phorbol 13-acetate 12-myristate (TPA) as an inducer of NF- kB signaling and positive control. We found that TPA induced 5-9-fold NF-kB activation, while 10S-E2 was the most effective in reducing NF-kB activity in K562 cells, inhibiting luciferase activity by 60%. In Granta cells, 10S-E2 inhibited luciferase activity by 15%, but this decrease was not statistically significant. Data on 4S-C2 and 8S-E3 were controversial; thus, 4S-C2 significantly decreased NF-kB activity in Granta cells but induced it in K562 cells (Figure 4A).

The 10S-E2 effects on NF-kB signaling were further confirmed by Q-PCR analysis, demonstrating the downregulation of GR TR marker genes: interleukins IL1-$\alpha$ and IL6 involved in lymphoid cell survival and inflammatory response [32,44–46] (Figure 4B).

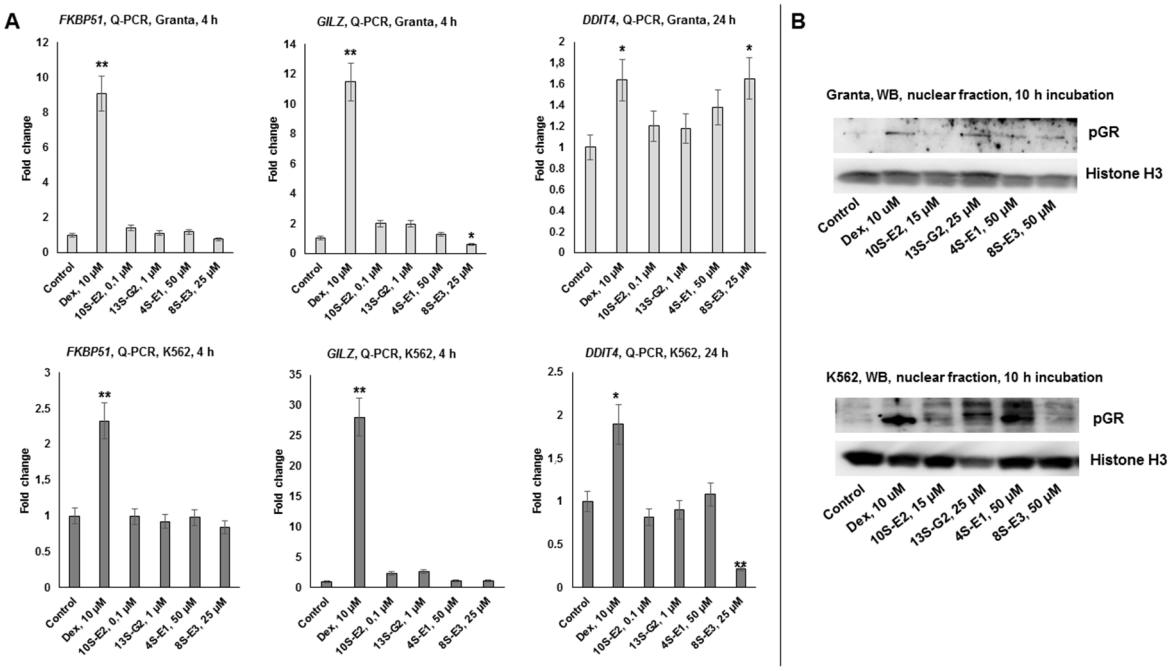


**Figure 3.** Effects of synephrine derivatives on GR transactivation in lymphoma and leukemia cells. (**A**) Q-PCR analysis of *FKBP51, GILZ,* and *DDIT4* mRNA expression in K562 and Granta cells. Cells were treated with Dex

 doi:10.20944/preprints202510.1879.v1



(10 μM), 4S-C2 (50 μM), 8S-E3 (25 μM), 10S-E2 (0.1 μM), 13S-G2, or vehicle for 4 h (*FKBP51, GILZ*) or 24 h (*DDIT4*). The Q-PCR results were normalized to the expression of the housekeeping gene RPL27 and are presented as fold changes compared to the control. The mean ± SD was calculated for three individual samples/condition. Statistically significant difference compared to the control: * - $p < 0.05$, ** - $p < 0.01$. (**B**) The levels of the nuclear fraction of phospho-GR (Ser211) were determined using Western blot analysis. Histone H3 was used as a loading control..

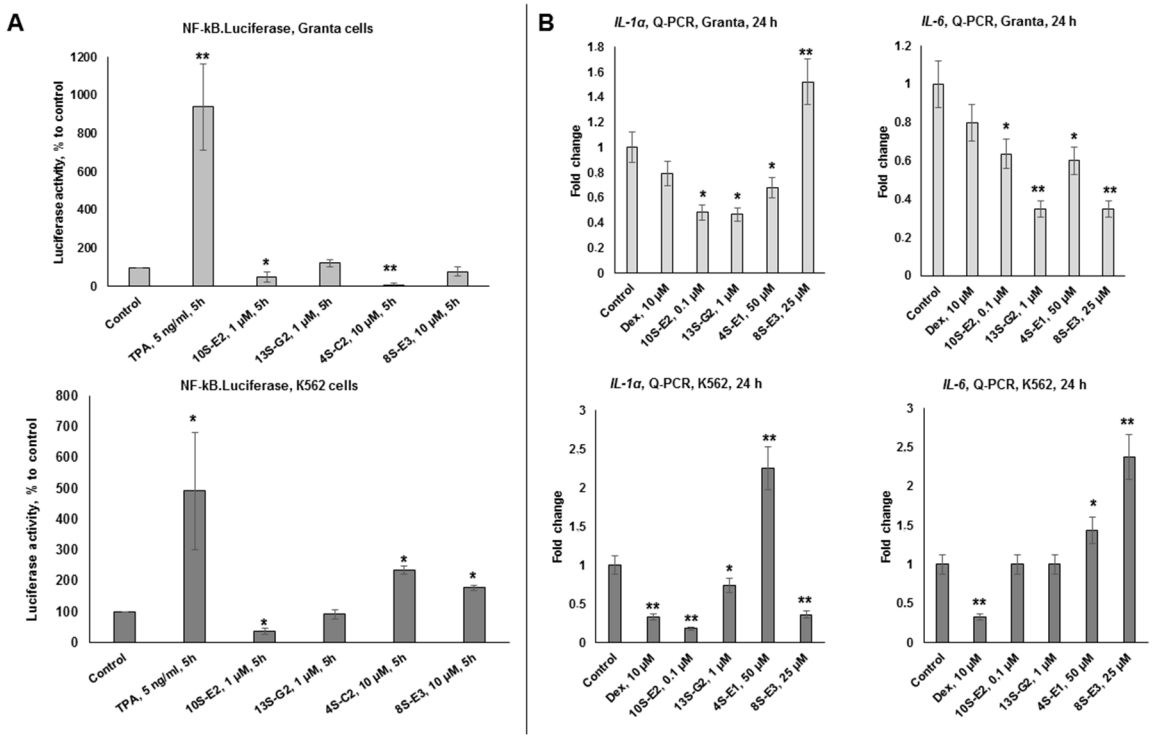


**Figure 4.** Effects of synephrine derivatives on GR transrepression in lymphoma and leukemia cells**.** (**A**) K562 and Granta cells stably infected with the lentiviruses bearing the NF-kB.Luciferase reporter. Cells were incubated for 5 h with the solvent (control), TPA (5 ng/ml), 4S-C2 (10 μM), 8S-E3 (10 μM), 10S-E2 (1 μM), or 13S-G2 (1 μM). Luciferase activity was determined as described in the Materials and Methods section. (**B**) *IL1-α* and *IL6* mRNA expression in K562 and Granta cells. Q-PCR results were normalized to the expression of the housekeeping gene RPL27 and are presented as fold change compared to the control. The mean ± SD was calculated for three individual samples/condition. Statistically significant difference compared to control: * - $p < 0.05$, ** - $p < 0.01$.

### *2.3. Anti-Apoptotic and Anti-Cancer Effects of Synephrine Derivatives In Vitro and In Vivo*

We examined the effects of 4S-C2, 8S-E3, 10S-E2, and 13S-G2 on cell cycle progression and apoptosis induction using flow cytometry. Cell cycle analysis showed that the level of apoptosis (the sub-G1-phase cell population) in Granta cells treated with the synephrine derivatives and Dex was higher than that in the control samples (Figure 5A). In the case of 10S-E2 treatment, a decrease in the number of cells in the G1 phase was observed in both cell lines. Interestingly, 10S-E2 did not induce apoptosis in K562 cells but increased the number of replicating cells in the S phase. This could reflect the different origins of the cells, followed by fluctuations in signaling and response to treatment.

Overall, 10S-E2 was the most active compound among the 26 synephrine derivatives and was tested in pilot experiments *in vivo* on a transplantable tumor lymphoma P388 model (Figure 5B) and ex vivo using primary lymphoblasts from pediatric patients with acute lymphoblastic leukemia (ALL) (Table 2). We found that inhibition of tumor growth in the animals treated with Dex (1 mg/kg) and 10S-E2 (10 mg/kg) was approximately 60-70% with the Dex superiority (Figure 5B). Toxicity was monitored through general cage observations and weight monitoring. The $IC_{50}$ values of 10S-E2 evaluated in primary lymphoblast samples from 19 patients diagnosed with ALL ranged from 40 to

 doi:10.20944/preprints202510.1879.v1



70 μM (Table 2). This could reflect the lower sensitivity of lymphoblasts derived from patients in the blast crisis stage. Dosage regimens should also be developed and optimized.

**Table 2.** The $IC_{50}$ values of 10S-E2 cytotoxic effects in primary lymphoblasts from the pediatric patients with acute lymphoblastic leukemia.

| No | Patient Code | $IC_{50}$, μM |
|---|---|---|
| 1 | 3 | 40.9±3.12 |
| 2 | 4 | 43.2±9.48 |
| 3 | 7 | 43.0±0.71 |
| 4 | 8 | 60.6±0.97 |
| 5 | 10 | 71.3±5.59 |
| 6 | 12 | 75.7±4.63 |
| 7 | 20 | 64.2±0.55 |
| 8 | 21 | 49.4±1.95 |
| 9 | 23 | 55.2±2.25 |
| 10 | 24 | 70.3±2.54 |
| 11 | 25 | 80.3±4.09 |
| 12 | 30 | 52.4±0.07 |
| 13 | 31 | 63.2±1.42 |
| 14 | 33 | 67.6±4.02 |
| 15 | 34 | 55.0±1.91 |
| 16 | 35 | 65.9±0.27 |
| 17 | 37 | 69.8±3.66 |
| 18 | 39 | 71.3±2.59 |
| 19 | 46 | 71.5±2.08 |

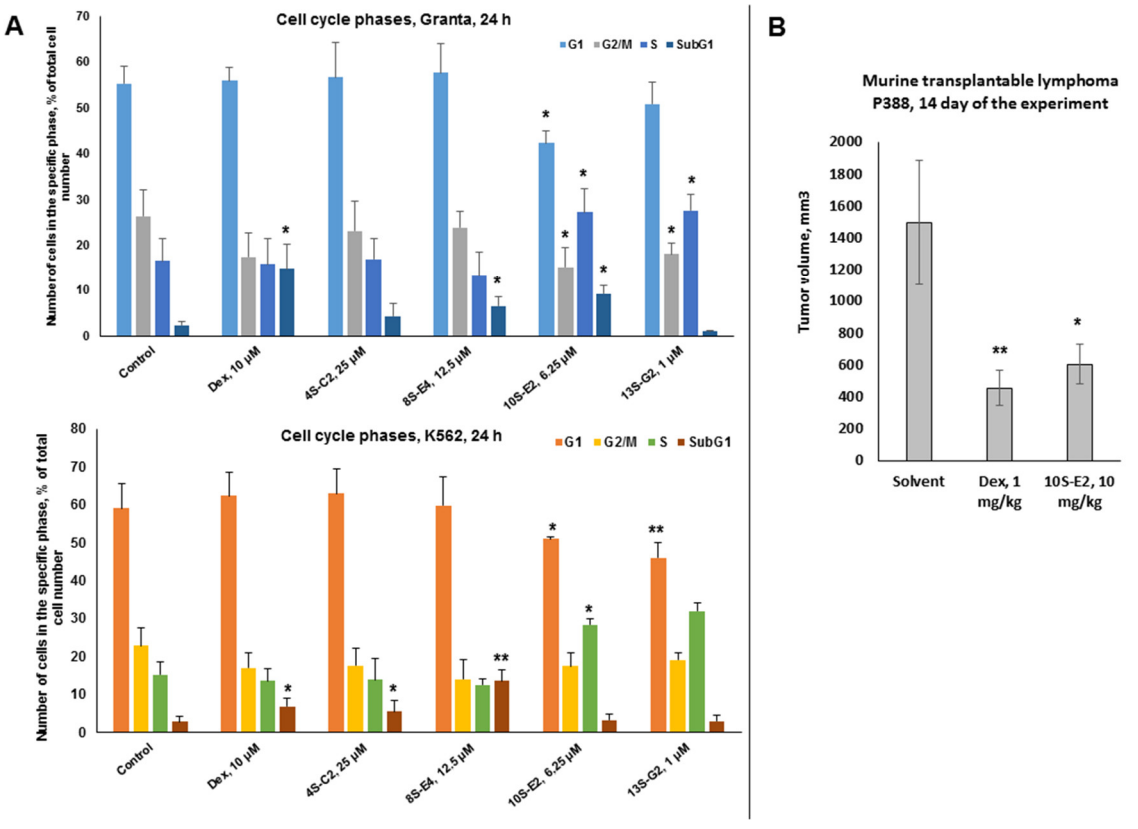


**Figure 5.** Anti-apoptotic and anti-cancer effects of synephrine derivatives in vitro and in vivo. **A**. Effect of 4S-C2, 8S-E3, 10S-E2 and 13S-G2 on cell cycle progression in K562 and Granta cells after 24 h of incubation. The cells were fixed with ethanol, stained with propidium iodide, and analyzed using flow cytometry. Statistically

 doi:10.20944/preprints202510.1879.v1



significant difference compared to control: * - $p < 0.05$, ** - $p < 0.01$. **B**. In vivo anticancer activity was evaluated using the transplantable P388 murine lymphoma model. Animals were treated i.p. 3 times per week with Dex (1 mg/kg), 10S-E2 (10 mg/kg) or solvent (ethanol:tween 80:distilled water=0.5:0.5:9). Tumor nodule size was measured twice a week using digital calipers. Statistically significant difference compared to control: * - $p < 0.05$, ** - $p < 0.01$.

*2.4. 10S-E2 Did Not Induce the Atrophic Changes in Skin and Bone Tissue as Compared to Dex*

We selected 10S-E2, which most significantly modulated GR function and displayed anti-cancer effects both *in vitro* and *in vivo*, to test its possible atrophogenic effect in skin and bone. 10S-E2 is GR ligand, and the activated receptor could act in pleotropic manner depending on tissue affected *[33,47–49]*. To test whether 10S-E2 could avoid the atrophogenic action of GC, we optimized previously described model of GC-induced osteoporosis in Balb/c female mice [36,47,50], formed the group of animals with pathology, and assessed atrophy in both bone and skin induced by high-dose i.p. Dex injections (20 mg/kg) were administered every 48 h for 6 weeks. 10S-E2 (10 mg/kg) or vehicle were injected to animals in experimental and control groups. Animal weight and behaviour was similar between the control and experimental groups. We observed a significant decrease in femoral bone thickness between animals in the control and Dex-treated groups, whereas 10S-E2 did not cause any loss in bone thickness (Figure 6A). Moreover, this observation was supported with Q-PCR data on the expression of known osteoporosis and cellular matrix degradation marker genes: Rankl (associated with bone resorption) [51], Trap (marker of osteoclast activity), Mmp9 (cellular matrix degrader) [52,53], Tsc2 (hypoxia-induced negative regulator of proliferation) [54], and Bglap (osteogenic marker) [55,56]. Downregulation of Bglap, upregulation of Rankl and Trap, and a tendency to Mmp9 and Tsc2 upregulation clearly proved osteoporosis development in Dex-treated animals (Figure 6B). In contrast, 10S-E2 significantly downregulated Rankl, Tsc2, Mmp9, and Trap compared to Dex and the control (Figure 6B).

To test whether 10S-E2 could induce the development of skin atrophy as a GR-activating ligand, we assessed morphological changes in the skin of Balb/c female mice. In agreement with previously published results [47], chronic treatment with systemic Dex led to a significant cutaneous atrophy, with dermal adipose tissue reduced by approximately 70% (Figure 6C). At the same time, 10S-E2 preserved the skin architecture, similar to that of the control group (Figure 6C).

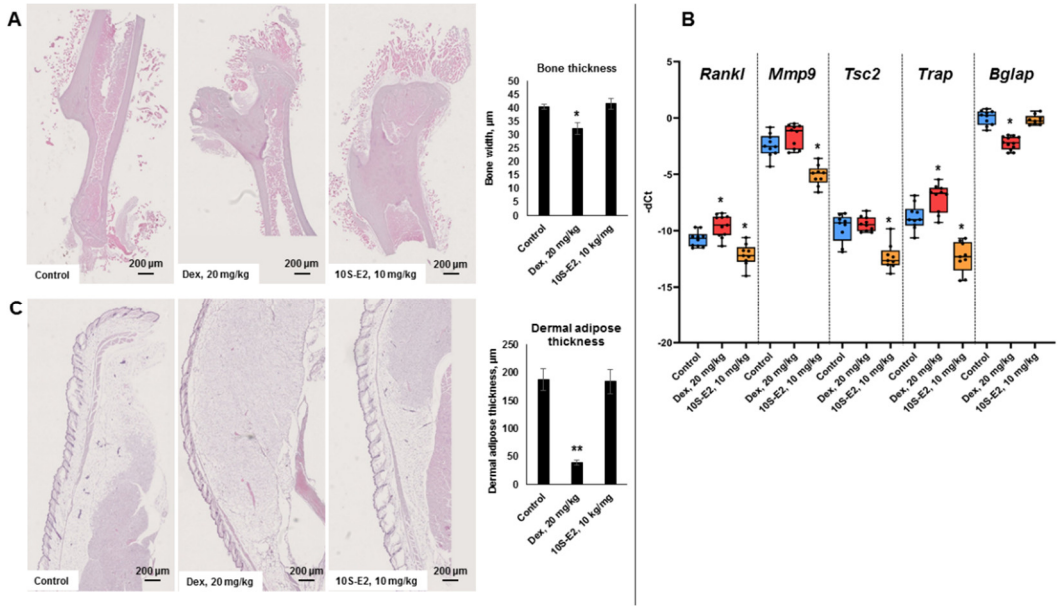


**Figure 6.** 10S-E2 did not induce atrophic changes in the skin and bone tissue compared to Dex. 10 weeks old female BALB/c mice (10/group) were treated every 24 h with i.p. injections for 5 weeks with Dex (20 mg/kg), 10S-E2 (10 mg/kg) and the solvent (ethanol:tween 80:distilled water=0.5:0.5:9). (**A**) H&E bone staining and

 doi:10.20944/preprints202510.1879.v1



quantification of cortical bone thickness. (**B**) Q-PCR analysis of *Rankl, Mmp9, Tsc2, Trap,* and *Bglap* mRNA expression in bone tissue. The Q-PCR results (for three individual RNA samples/condition) were normalized to the expression of the housekeeping gene *Rpl27* and presented as fold change compared to the control. (**C**) H&E skin staining and quantification of dermal adipose thickness. Statistically significant difference compared to control: * - $p < 0.05$, ** - $p < 0.01$.

## 3. Discussion

Glucocorticoids are involved in the regulation of different physiological processes modulating numerous and multidirectional signals. The search for GC alternatives with a similar spectrum of clinically demanded anti-proliferative and anti-inflammatory actions but with attenuated side effects is urgently needed for thousands of patients. Preservation of therapeutically important GR TR could be reached by using a combination of GCs with tissue protectors against metabolic and atrophic complications [16,32,33,42]. Another option assumes the design of selective glucocorticoid receptor agonists/modulators (SEGRAM) that shift GR activity towards TR and could serve as GC alternatives with an improved therapeutic index, referring to the ratio between the mean toxic dose associated with side effects and effective dose [16,18,57–64].

Previously, we developed and described the derivatives of Compound A (CpdA), a widely characterized molecule from the SEGRAM class, 4-(1-hydroxy-2-(piperidin-1-yl)ethyl)phenol or CpdA-03, demonstrating superior biological activity compared to CpdA [14]. The second strategy for the development of novel SEGRAM was the use of the synephrine molecule as a template for SEGRAM design [30]. The approach for the development of novel SEGRAM on the template of compounds of natural origin, with anti-inflammatory activity comparable to that of GC, was described for boswellic acids and their derivatives. The mentioned boswellic acid derivatives originated from natural sources without any synthetic modification of the boswellic acid molecule [65]. Our approach, based on the chemical modification of naturally occurring proven or potential SEGRAM, is still pioneering in the field of novel partial GR agonists.

Preliminary screening of the cytotoxic effects revealed 10S-E2 and 13S-G2 as leader compounds with the highest affinity to GR *in silico* and *in vitro* (Figure 2 and [30]), which was in line with the pronounced inhibitory effects on the expression of GR-regulated proliferative and inflammatory genes (GR TR, Figure 4) and the absence of GR TA induction (Figure 3). The divergent effects of 8S-E3, 4S-C2, and 13S-G2 on gene expression patterns, as well as their moderate cytotoxic activity, make these three compounds less promising for further analysis. Therefore, 10S-E2 is the most prominent molecule for further preclinical studies and pharmaceutical development.

Furthermore, it was demonstrated that the lead compound, 10S-E2, exhibited cytotoxic effects at concentrations of 10-20 μM in mantle cell lymphoma Granta and chronic myeloleukemia K562 cells and at concentration of 40-70 μM in primary PBMC from the patients with ALL, together with the induction of apoptosis in Granta cells (Figure 5 and [30]), which exceeded the moderate cytotoxicity of the template molecule, synephrine [66–68]. The anti-cancer effects of 10S-E2 *in vivo*, compared to the reference drug Dex, could be associated with GR TR activation and did not lead to the development of GC-induced resistance [69,70]. Moreover, the absence of atrophic effects in the glucocorticoid-induced osteoporosis model demonstrated the safety profile of the molecule (Figure 6). Further studies should be conducted to evaluate the possible protective effects of 10S-E2 in combination with GCs. Similar studies of protective effects were earlier reported for ginsenoside Rg1, a selective glucocorticoid receptor agonist of natural origin [28,29].

## 4. Materials and Methods

### *4.1. Cells and Treatments*

Chronic myeloid leukemia cell line K562 and mantle cell lymphoma cell line Granta were obtained from ATCC and cultured in RPMI-1640 medium (“Paneco”, Russia) supplemented with a

 doi:10.20944/preprints202510.1879.v1



10% fetal bovine serum (“Biowest”, France), 2 mM L-glutamine, 5 ME/mL penicillin and 5 μg/mL streptomycin (“Paneco”, Russia) at 37 °C and 5% $CO_2$ as described [19].

Cells were treated with dexamethasone (Dex) (“Macklin”, China), CpdA, 4S-C2, 8S-E3, 10S-E2, and 13S-G2 synthesized as described [30], or vehicle (0.01% DMSO unless other specified).

*4.2. Cell Cycle Analysis*

The distribution of cells by cell cycle phases was evaluated using propidium iodide (PI) staining, as described in [19]. Cells were seeded into 24-well plates ($10^5$ cells/well) and treated with Dex (50 μM), 4S-C2 (25 μM), 8S-E3 (12.5 μM), 10S-E2 (6.25 μM), 13S-G2 (1 μM), or the vehicle for 24 h. After incubation, the cells were resuspended in 70% ethanol and fixed for 2h at 4°C. Cells were then washed twice with cold PBS, pH 7.4, and stained with 500 μL of cold propidium iodide (PI) solution (50 μg/mL PI, 1% Triton X-100, and 100 μg/mL RNase A in PBS). The cell cycle distribution of cells in samples were analyzed using a FACSCalibur Flow Cytometer (“BD Biosciences”, USA).

*4.3. Western Blot Analysis*

Cells were seeded into 24-well plates ($10^5$ cells/well) and treated with Dex (10 μM), 4S-C2 (50 μM), 8S-E3 (50 μM), 10S-E2 (15 μM), 13S-G2 (25 μM), or the vehicle for 10 h. Western blot analysis was performed as previously described [19,31]. Proteins were resolved using SDS-PAGE. Membranes were blocked with 5% nonfat milk solution and then incubated with primary antibodies against phosphorylated GR (pGR, Ser211) (“Santa Cruz Biotechnology”, USA) overnight at 4°C. To verify equal protein loading and adequate transfer, the membranes were probed with Histone H3 antibodies (“Cell Signaling”, USA). Goat anti-rabbit IgGs (“Jackson Immuno Research”, USA) were used as secondary antibodies. Signals were detected using ECL reagent and an ImageQuant LAS4000 system (“GE HealthCare”, USA). ImageJ software was used for densitometry. Each point was tested in two technical and three biological replicates.

*4.4. Human Peripheral Blood Mononuclear Cell (PBMC) Isolation and Culture*

Peripheral blood samples were collected from 1–10-year-old pediatric patients with newly diagnosed T-ALL in the acute phase of the disease at N.N. Blokhin National Research Center of Oncology. The Ethical Committee of the N.N. Blokhin National Research Center of Oncology approved this study, and the parents or guardians of the patients provided written informed consent. Monocytes were isolated by centrifugation with Ficoll-Isopaque (“Paneco”, Russia) and then cultured in the RPMI-1640 media (“Paneco”, Russia) supplemented with 20% FBS (“Biowest”, France), 2 mM L-glutamine, 0.5 ME/mL penicillin and 0.5 μg/mL streptomycin (“Paneco”, Russia), 10 mg/L phytohaemagglutinin (“Paneco”, Russia).

*4.5. Resazurin Cytotoxicity Assay*

Isolated PBMC were seeded into 96-well plates ($2\times10^6$ cells/well) and treated with 10S-E2 at a wide range of concentrations (2-200 μM). Cell viability was analyzed after 24 h of incubation, assessing metabolic activity with the addition of 0.177 mg/ml of resazurin at 8-10 h before the end of the incubation. Fluorescence intensity was evaluated using a Fluoroskan FL microplate fluorimeter (“Thermo Scientific”, USA). The $IC_{50}$ values were determined using GraphPad Prism software version 8.2.1. Each point was tested in two technical and three biological replicates.

*4.6. RNA Extraction and Q-PCR*

Total RNA isolation from cell cultures and murine bones, reverse transcription, and Q-PCR were performed as described in [32]. Primers were designed using NCBI Primer-BLAST (Supplementary Table S1). Results were normalized to the expression of the housekeeping *RPL27* и *Rpl27* genes [32,33].

 doi:10.20944/preprints202510.1879.v1



*4.7. Lentivirus Preparation and Cell Transduction*

Lentiviral stocks were generated using lentiviral expression vector NF-kB.Luc was encoded Firefly Luciferase reporters under NF-kB responsive promoter of minimal CMV promoter as control ("System Bioscience", USA) along with packing plasmids GAG, REV and VSVg [14,34]. HEK-293T cells were transfected with abovementioned plasmids using TurboFect reagent ("Thermo Scientific", USA) according to the manufacturer's protocol. Viral stocks were collected after 24-48 h after transfection, sterilized by 0.2 μm filtration, and applied to K562 and Granta cells for 24 h. K562 and Granta cells infected with lentiviruses were selected using 0.5 μg/ml puromycin.

*4.8. Luciferase Assay*

Cells ($10^4$ cells/well in 24-well plate), stably expressing Firefly Luciferase under NF-kB -promoter, were treated for 5 h with TPA (12-O-tetradecanoylphorbol-13-acetate, "Cell Signaling", USA, 10 ng/ml), 4S-C2 (10 μM), 8S-E3 (10 μM), 10S-E2 (1 μM), 13S-G2 (1 μM) or vehicle. Luciferase activity was measured as described [32,33] using a commercial Luciferase Assay (Promega) and Luminometer TD 20/20 (Turner Design Instruments). Cells stably expressing Firefly Luciferase under the minimal CMV promoter were used as a control to adjust for nonspecific toxicity. The results were normalized to the total protein amount in each sample.

*4.9. Molecular Docking and Molecular Dynamics Simulation*

Ligand structures were prepared using ChemDraw 17.0 software. Molecular docking was performed using the SwissDock online server (http://old.swissdock.ch), and the results were analyzed using UCSF Chimera 1.16. Blind docking resulted in 250 models for each compound, which were grouped into 35-45 clusters. Cluster 0 was selected for further analysis. The stability of the complex was studied using molecular dynamics simulations in GROMACS. The loading file for the calculations was prepared using the CHARMM-GUI generator (https://www.charmm-gui.org). Because the binding of the receptor to the ligand occurs in the cytoplasm, basic solution conditions were selected for the simulation. Molecular dynamics calculations in GROMACS were performed with a time step of 0.002 ps, and the coordinates were recorded every 5000 steps. The trajectory lengths were 4 and 10 ns. The obtained trajectories were analyzed using VMD 2.0.0a7.

*4.10. GR Binding Affinity Assay*

K562 cells ($2.5x10^6$ cells/ml) were cultured in a serum-free culture medium in the presence of 0.5 μM [3H]Dex and unlabeled Dex, CpdA, 4S-C2, 8S-E3, 10S-E2, and 13S-G2 at various concentrations. After 90 min of incubation, the cells were washed twice by centrifugation in cold serum-free medium (1500 rpm, 5 min). The cells were then lysed with RIPA buffer (50 mM Tris (pH 8.0), 150 mM NaCl, 1 mM ethylenediaminetetraacetic acid, 0.1% sodium dodecyl sulfate, 0.5% sodium deoxycholate, 1% triton-X100, 10% glycerin, and protease inhibitor) for 20 min. Lysates were transferred to scintillation liquid, and radioactivity was measured using a RackBeta 1215 LC spectrometer for 4 min. The relative binding percentages of Dex, CpdA, 4S-C2, 8S-E3, 10S-E2 and 13S-G2were measured. $IC_{50}$ was determined using GraphPad Prism software, Ver.7.0. Measured values represented in decay per minute (dpm) of different concentrations of Dex were calculated using a method of non-linear regression (curve fit) with the equation - [Inhibitor] vs response (three parameters: «top», «bottom», $IC_{50}$). «Top» meant the highest value in dpm and was equal to 100%, while the «bottom» was considered as the lowest value (0%). Dpm for 4S-C2, 8S-E3, 10S-E2, and 13S-G2 were calculated in the same way using the «bottom» of Dex in the individual biological repeat. These calculations led to plotting curves that most precisely fit the pattern of competitive inhibition by a ligand of binding [3H]Dex to GR. The $IC_{50}$ values for each ligand were determined by plotting these curves.

*4.11. Anti-Cancer Study In Vivo*

 doi:10.20944/preprints202510.1879.v1



The protocol for the experiment was approved by the local N.N. Blokhin National Medical Research Center Ethics Committee and corresponded to the guidelines for the welfare and use of animals in cancer research adopted by The United Kingdom Coordinating Committee on Cancer Prevention Research [35]. P388 cells were injected i.p. into 5 weeks old female DBA/2 mice ("Stolbovaya Farm", Russia). After 15 days, the cells were collected from the peritoneum, washed, and resuspended in PBS. For the experiments, 0.1 ml containing 2 million cells obtained from the ascites was inoculated s.c. in 5 weeks old female BDF1 mice ("Stolbovaya Farm", Russia). Mice were randomly divided into three groups, 10 animals per group, and treated i.p. 3 times/week with Dex (1 mg/kg), 10S-E2 (10 mg/kg) or with the solvent (ethanol:tween 80:distilled water=0.5:0.5:9). Body weight was recorded twice a week for toxicity determination. Tumor size was measured three times per week using digital calipers.

### *4.12. Glucocorticoid-Induced Osteoporosis*

The protocol for the experiment was approved by the local N.N. Blokhin National Medical Research Center Ethics Committee and corresponded to the guidelines for the welfare and use of animals in cancer research adopted by The United Kingdom Coordinating Committee on Cancer Prevention Research [35]. 10 weeks old BALB/c female mice ("Stolbovaya-farm", Russia) were randomly divided into three groups, 10 animals per group, and treated i.p. every 24 h for 5 weeks with Dex (20 mg/kg) for glucocorticoid-induced osteoporosis (GIOP) as described [36], 10S-E2 (10 mg/kg) and the solvent (ethanol:tween 80:distilled water=0.5:0.5:9). Body weight was recorded twice a week for toxicity control.

### *4.13. Histology and Morphometry*

Bone and skin samples from the GIOP experiment were fixed in formaldehyde, embedded in paraffin, and sections were stained with hematoxylin and eosin. After formaldehyde fixation, the bone samples were decalcified in decalcification buffer (0.5 M EDTA, 0.7 mM NaOH, pH7.0) for 14 days, washed twice with PBS, and further processed according to the standard histology protocol. The dermal adipose and bone thickness were quantified in sections stained with hematoxylin and eosin. At least five individual fields per slide of each sample/treatment (at least 50 images/treatment group) were analyzed using the Axioplan2 microscope software (Carl Zeiss). The dermal adipose or bone thickness in treated animals is presented as a percentage of control animals.

### *4.14. Statistical Analysis*

Mean and standard deviation values were calculated using Microsoft Excel and GraphPad Prism (Ver.7.0) software. The treatment effects in each experiment were compared using one-way ANOVA or t-test. Differences between groups were considered significant at $p<0.05$.

## 5. Conclusions

In this study, we investigated the biological effects of novel GR ligands from the class of synephrine derivatives and demonstrated the anti-cancer effect of 1-[4-(benzyloxy)phenyl]-2-(hexylamino)ethanol (10S-E2) in vitro, in vivo, and ex vivo. Moreover, for 10S-E2, we showed the absence of GR transactivation, resulting in the preservation of bone and skin tissues during long-term treatment. This fact gives the advantage to 10S-E2 as a GR ligand with anti-cancer properties and a higher safety profile, and proposes to combine this synephrine derivative with GCs to study potential protective effect of 10S-E2.

**Supplementary Materials:** The following supporting information can be downloaded at the website of this paper posted on Preprints.org, Zhidkova et al., Supplementary Material.

**Author Contributions:** Conceptualization, E.M.Zh., A.V.M., S.A.D., A.A.K., T.T.V., M.G.Y., E.A.L.; methodology, E.M.Zh., A.V.M., M.G.C., D.V.M., O.A.V., A.D.E., G.A.B., S.A.D., A.A.K., E.A.Yu., K.V.G., D.V.M.;

 doi:10.20944/preprints202510.1879.v1



software, E.D.S., A.V.M., E.A.Yu., K.V.G., E.M.Zh., A.D.E.; investigation, E.D.S., A.V.M., E.A.Yu., M.G.C., K.V.G., E.M.Zh., A.D.E., O.A.V., P.A.K., D.V.M., S.A.D., A.A.K., E.A.L.; resources, E.A.Yu., T.T.V., A.V.M., M.G.C., M.G.Y., G.A.B., S.A.D., A.A.K., E.A.L.; writing—original draft preparation, E.A.L.; writing—review and editing, E.M.Zh., E.A.Yu., M.G.Y., S.A.D., A.A.K., T.T.V., E.A.L.; visualization, E.D.S., E.A.Yu., E.M.Zh., A.D.E., E.A.L.; supervision, E.A.L.; project administration, E.A.L.; funding acquisition, E.A.L. All authors have read and agreed to the published version of the manuscript.

**Funding:** The work was funded by Russian Science Foundation, grant number 23-15-00321 (to E.A.L.).

**Institutional Review Board Statement:** The animal study protocol and the protocol of the study using primary human PBMC were conducted in accordance with the Declaration of Helsinki, and approved by local N.N. Blokhin National Medical Research Center Ethics Committee (protocol code No2025-2c, 15.04.2025).

**Informed Consent Statement:** Informed consent was obtained from all subjects involved in the study.

**Data Availability Statement:** The original contributions presented in the study are included in the article and Supplementary Material, further inquiries can be directed to the corresponding author.

**Conflicts of Interest:** The authors declare no conflicts of interest.

## Abbreviations

The following abbreviations are used in this manuscript:

| | |
|---|---|
| ALL | acute lymphoblastic leukemia |
| BGLAP | bone gamma-carboxyglutamic acid-containing protein |
| CMV | cytomegalovirus |
| CpdA | compound A |
| DDIT4 | DNA-damage-inducible transcript 4 |
| Dex | dexamethasone |
| FKBP51 | FK506-binding protein 51 |
| GC | glucocorticoid |
| GILZ | glucocorticoid-induced leucine zipper |
| GIOP | glucocorticoid-induced osteoporosis |
| GR | glucocorticoid receptor |
| GRE | glucocorticoid-responsive elements |
| H&E | hematoxylin eosin |
| HEK | human embryonic kidney |
| $IC_{50}$ | 50% inhibitory concentration |
| IL1-$\alpha$ | interleukin 1-$\alpha$ |
| IL6 | interleukin 6 |
| MMP9 | matrix metalloproteinase-9 |
| PBMC | peripheral bone marrow cells |
| Q-PCR | quantitative polymerase chain reaction |
| RANKL | receptor activator of nuclear factor kappa-B |
| RMSD | root mean square deviation |
| RPL27 | ribosomal protein 27 |
| SEGRAM | selective glucocorticoid receptor agonist/modulator |
| TA | transactivation |
| TPA | 12-O-tetradecanoylphorbol-13-acetate |
| TR | transrepression |
| TRAP | tartrate-resistant acid phosphatase |
| TSC2 | tuberoses sclerosis complex 2 |

## References

1. Buttgereit, F. Views on Glucocorticoid Therapy in Rheumatology: The Age of Convergence. *Nat Rev Rheumatol* **2020**, *16*, 239–246, doi:10.1038/s41584-020-0370-z.

 doi:10.20944/preprints202510.1879.v1




2. Sundahl, N.; Bridelance, J.; Libert, C.; De Bosscher, K.; Beck, I.M. Selective Glucocorticoid Receptor Modulation: New Directions with Non-Steroidal Scaffolds. *Pharmacology & Therapeutics* **2015**, *152*, 28–41, doi:10.1016/j.pharmthera.2015.05.001.
3. Eiers, A.-K.; Vettorazzi, S.; Tuckermann, J.P. Journey through Discovery of 75 Years Glucocorticoids: Evolution of Our Knowledge of Glucocorticoid Receptor Mechanisms in Rheumatic Diseases. *Ann Rheum Dis* **2024**, ard-2023-225371, doi:10.1136/ard-2023-225371.
4. Cain, D.W.; Cidlowski, J.A. Specificity and Sensitivity of Glucocorticoid Signaling in Health and Disease. *Best Practice & Research Clinical Endocrinology & Metabolism* **2015**, *29*, 545–556, doi:10.1016/j.beem.2015.04.007.
5. Jakob, F.; Hennen, S.; Gautrois, M.; Khalil, F.; Lockhart, A. Novel Selective Glucocorticoid Receptor Modulator GRM-01 Demonstrates Dissociation of Anti-Inflammatory Effects from Adverse Effects on Glucose and Bone Metabolism. *Front. Pharmacol.* **2025**, *16*, 1542351, doi:10.3389/fphar.2025.1542351.
6. Li, J.-X.; Cummins, C.L. Fresh Insights into Glucocorticoid-Induced Diabetes Mellitus and New Therapeutic Directions. *Nat Rev Endocrinol* **2022**, *18*, 540–557, doi:10.1038/s41574-022-00683-6.
7. Van Staa, T.P. The Pathogenesis, Epidemiology and Management of Glucocorticoid-Induced Osteoporosis. *Calcif Tissue Int* **2006**, *79*, 129–137, doi:10.1007/s00223-006-0019-1.
8. De Bosscher, K.; Haegeman, G. Minireview: Latest Perspectives on Antiinflammatory Actions of Glucocorticoids. *Molecular Endocrinology* **2009**, *23*, 281–291, doi:10.1210/me.2008-0283.
9. Targeting Steroid Hormone Receptors for Anti-Cancer Therapy. In *Vitamins and Hormones*; Elsevier, 2025; Vol. 129, pp. 1–59 ISBN 978-0-443-29548-5.
10. Permpoon, U.; Moon, J.; Kim, C.Y.; Nam, T. Glucocorticoid-Mediated Skeletal Muscle Atrophy: Molecular Mechanisms and Potential Therapeutic Targets. *IJMS* **2025**, *26*, 7616, doi:10.3390/ijms26157616.
11. Pufall, M.A. Glucocorticoids and Cancer. In *Glucocorticoid Signaling*; Wang, J.-C., Harris, C., Eds.; Advances in Experimental Medicine and Biology; Springer New York: New York, NY, 2015; Vol. 872, pp. 315–333 ISBN 978-1-4939-2894-1.
12. Lucafò, M.; Franzin, M.; Decorti, G.; Stocco, G. A Patent Review of Anticancer Glucocorticoid Receptor Modulators (2014-Present). *Expert Opinion on Therapeutic Patents* **2020**, *30*, 313–324, doi:10.1080/13543776.2020.1740206.
13. Scheijen, B. Molecular Mechanisms Contributing to Glucocorticoid Resistance in Lymphoid Malignancies. *CDR* **2019**, doi:10.20517/cdr.2019.29.
14. Zhidkova, E.M.; Tilova, L.R.; Fetisov, T.I.; Kirsanov, K.I.; Kulikov, E.P.; Enikeev, A.D.; Budunova, I.V.; Badun, G.A.; Chernysheva, M.G.; Shirinian, V.Z.; et al. Synthesis and Anti-Cancer Activity of the Novel Selective Glucocorticoid Receptor Agonists of the Phenylethanolamine Series. *Int J Mol Sci* **2024**, *25*, 8904, doi:10.3390/ijms25168904.
15. Hsu, S.-J.; He, M.; Salomé-Abarca, L.F.; Choi, Y.H.; Wang, M. Uncovering Anti-Inflammatory Activity of Ginsenoside Rg1 in a Wound-Inured Zebrafish Model by GC-MS-Based Chemical Profiling. *Planta Med* **2025**, *91*, 609–620, doi:10.1055/a-2606-6705.
16. Lesovaya, E.A.; Chudakova, D.; Baida, G.; Zhidkova, E.M.; Kirsanov, K.I.; Yakubovskaya, M.G.; Budunova, I.V. The Long Winding Road to the Safer Glucocorticoid Receptor (GR) Targeting Therapies. *Oncotarget* **2022**, *13*, 408–424, doi:10.18632/oncotarget.28191.
17. Zhidkova, E.M.; Lylova, E.S.; Savinkova, A.V.; Mertsalov, S.A.; Kirsanov, K.I.; Belitsky, G.A.; Yakubovskaya, M.G.; Lesovaya, E.A. A Brief Overview of the Paradoxical Role of Glucocorticoids in Breast Cancer. *Breast Cancer (Auckl)* **2020**, *14*, 1178223420974667, doi:10.1177/1178223420974667.
18. Lesovaya, E.; Yemelyanov, A.; Swart, A.C.; Swart, P.; Haegeman, G.; Budunova, I. Discovery of Compound A - a Selective Activator of the Glucocorticoid Receptor with Anti-Inflammatory and Anti-Cancer Activity. *Oncotarget* **2015**, *6*, 30730–30744, doi:10.18632/oncotarget.5078.
19. Lesovaya, E.; Yemelyanov, A.; Kirsanov, K.; Popa, A.; Belitsky, G.; Yakubovskaya, M.; Gordon, L.I.; Rosen, S.T.; Budunova, I. Combination of a Selective Activator of the Glucocorticoid Receptor Compound A with a Proteasome Inhibitor as a Novel Strategy for Chemotherapy of Hematologic Malignancies. *Cell Cycle* **2013**, *12*, 133–144, doi:10.4161/cc.23048.
20. Buttgereit, F.; Elling, C.; Jakob, F. Design and Development of Glucocorticoid Receptor Modulators. *Trends in Pharmacological Sciences* **2025**, *46*, 771–791, doi:10.1016/j.tips.2025.06.005.

 doi:10.20944/preprints202510.1879.v1




21. Brown, M.N.; Fuhr, R.; Beier, J.; Su, H.-L.; Chen, Y.; Forsman, H.; Hamrén, U.W.; Jackson, H.; Aggarwal, A. Efficacy and Safety of AZD7594, an Inhaled Non-Steroidal Selective Glucocorticoid Receptor Modulator, in Patients with Asthma: A Phase 2a Randomized, Double Blind, Placebo-Controlled Crossover Trial. *Respir Res* **2019**, *20*, 37, doi:10.1186/s12931-019-1000-7.
22. Cheng, F.; Shen, T.; Zhang, F.; Lei, C.; Zhu, Y.; Luo, G.; Xiao, D. Bioequivalence Study of Fluticasone Propionate Nebuliser Suspensions in Healthy Chinese Subjects. *Front. Pharmacol.* **2025**, *15*, 1452596, doi:10.3389/fphar.2024.1452596.
23. Hunt, H.; Donaldson, K.; Strem, M.; Zann, V.; Leung, P.; Sweet, S.; Connor, A.; Combs, D.; Belanoff, J. Assessment of Safety, Tolerability, Pharmacokinetics, and Pharmacological Effect of Orally Administered CORT125134: An Adaptive, Double-Blind, Randomized, Placebo-Controlled Phase 1 Clinical Study. *Clinical Pharm in Drug Dev* **2018**, *7*, 408–421, doi:10.1002/cpdd.389.
24. Kuna, P.; Aurivillius, M.; Jorup, C.; Prothon, S.; Taib, Z.; Edsbäcker, S. Efficacy and Tolerability of an Inhaled Selective Glucocorticoid Receptor Modulator – AZD5423 – in Chronic Obstructive Pulmonary Disease Patients: Phase II Study Results. *Basic Clin Pharma Tox* **2017**, *121*, 279–289, doi:10.1111/bcpt.12768.
25. Werkström, V.; Prothon, S.; Ekholm, E.; Jorup, C.; Edsbäcker, S. Safety, Pharmacokinetics and Pharmacodynamics of the Selective Glucocorticoid Receptor Modulator AZD5423 after Inhalation in Healthy Volunteers. *Basic Clin Pharma Tox* **2016**, *119*, 574–581, doi:10.1111/bcpt.12621.
26. Conrado, D.J.; Krishnaswami, S.; Shoji, S.; Kolluri, S.; Hey-Hadavi, J.; McCabe, D.; Rojo, R.; Tammara, B.K. Predicting the Probability of Successful Efficacy of a Dissociated Agonist of the Glucocorticoid Receptor from Dose–Response Analysis. *J Pharmacokinet Pharmacodyn* **2016**, *43*, 325–341, doi:10.1007/s10928-016-9475-z.
27. Bareille, P.; Hardes, K.; Donald, A.C. Efficacy and Safety of Once-Daily GW870086 a Novel Selective Glucocorticoid in Mild-Moderate Asthmatics: A Randomised, Two-Way Crossover, Controlled Clinical Trial. *Journal of Asthma* **2013**, *50*, 1077–1082, doi:10.3109/02770903.2013.837480.
28. Fan, X.; Zhang, Y.; Li, X.; Ding, J.; Huang, J.; Lian, K.; Duan, P.; Hu, C.; Xu, J. Unraveling Ginsenoside Rg1's Osteoprotective Pathways in Zebrafish Models of Glucocorticoid Induced Osteoporosis via Transcriptomics. *Sci Rep* **2025**, *15*, 30519, doi:10.1038/s41598-025-15284-2.
29. Harcken, C.; Scholl, P.; Nabozny, G.; Thomson, D.; Bianchi, D. Clinical Profile of the Functionally Selective Glucocorticoid Receptor Agonist BI 653048 in Healthy Male Subjects. *Expert Opinion on Investigational Drugs* **2019**, *28*, 489–496, doi:10.1080/13543784.2019.1599859.
30. Zhidkova, E.M.; Oleynik, E.S.; Mikhina, E.A.; Stepanycheva, D.V.; Grigoreva, D.D.; Grebenkina, L.E.; Gordeev, K.V.; Savina, E.D.; Matveev, A.V.; Yakubovskaya, M.G.; et al. Synthesis and Anti-Cancer Activity In Vitro of Synephrine Derivatives. *Biomolecules* **2024**, *15*, 2, doi:10.3390/biom15010002.
31. Yemelyanov, A.; Czwornog, J.; Chebotaev, D.; Karseladze, A.; Kulevitch, E.; Yang, X.; Budunova, I. Tumor Suppressor Activity of Glucocorticoid Receptor in the Prostate. *Oncogene* **2007**, *26*, 1885–1896, doi:10.1038/sj.onc.1209991.
32. Lesovaya, E.; Agarwal, S.; Readhead, B.; Vinokour, E.; Baida, G.; Bhalla, P.; Kirsanov, K.; Yakubovskaya, M.; Platanias, L.C.; Dudley, J.T.; et al. Rapamycin Modulates Glucocorticoid Receptor Function, Blocks Atrophogene REDD1, and Protects Skin from Steroid Atrophy. *Journal of Investigative Dermatology* **2018**, *138*, 1935–1944, doi:10.1016/j.jid.2018.02.045.
33. Baida, G.; Bhalla, P.; Kirsanov, K.; Lesovaya, E.; Yakubovskaya, M.; Yuen, K.; Guo, S.; Lavker, R.M.; Readhead, B.; Dudley, J.T.; et al. REDD1 Functions at the Crossroads between the Therapeutic and Adverse Effects of Topical Glucocorticoids. *EMBO Mol Med* **2015**, *7*, 42–58, doi:10.15252/emmm.201404601.
34. Lesovaya, E.A.; Yemelyanov, A.Yu.; Kirsanov, K.I.; Yakubovskaya, M.G.; Budunova, I.V. Antitumor Effect of Non-Steroid Glucocorticoid Receptor Ligand CpdA on Leukemia Cell Lines CEM and K562. *Biochemistry Moscow* **2011**, *76*, 1242–1252, doi:10.1134/S000629791111006X.
35. Workman, P.; Aboagye, E.O.; Balkwill, F.; Balmain, A.; Bruder, G.; Chaplin, D.J.; Double, J.A.; Everitt, J.; Farningham, D. a. H.; Glennie, M.J.; et al. Guidelines for the Welfare and Use of Animals in Cancer Research. *Br J Cancer* **2010**, *102*, 1555–1577, doi:10.1038/sj.bjc.6605642.
36. McLaughlin, F.; Mackintosh, J.; Hayes, B.P.; McLaren, A.; Uings, I.J.; Salmon, P.; Humphreys, J.; Meldrum, E.; Farrow, S.N. Glucocorticoid-Induced Osteopenia in the Mouse as Assessed by Histomorphometry,

 doi:10.20944/preprints202510.1879.v1



Microcomputed Tomography, and Biochemical Markers. *Bone* **2002**, *30*, 924–930, doi:10.1016/S8756-3282(02)00737-8.

37. Brandon, D.D.; Kendall, J.W.; Alman, K.; Tower, P.; Loriaux, D.L. Inhibition of Dexamethasone Binding to Human Glucocorticoid Receptor by New World Primate Cell Extracts. *Steroids* **1995**, *60*, 463–466, doi:10.1016/0039-128x(95)00039-s.
38. Yemelyanov, A.; Czwornog, J.; Gera, L.; Joshi, S.; Chatterton, R.T.; Budunova, I. Novel Steroid Receptor Phyto-Modulator Compound a Inhibits Growth and Survival of Prostate Cancer Cells. *Cancer Res* **2008**, *68*, 4763–4773, doi:10.1158/0008-5472.CAN-07-6104.
39. Ronacher, K.; Hadley, K.; Avenant, C.; Stubsrud, E.; Simons, S.S.; Louw, A.; Hapgood, J.P. Ligand-Selective Transactivation and Transrepression via the Glucocorticoid Receptor: Role of Cofactor Interaction. *Molecular and Cellular Endocrinology* **2009**, *299*, 219–231, doi:10.1016/j.mce.2008.10.008.
40. Yang, N.; Baban, B.; Isales, C.M.; Shi, X.-M. Role of Glucocorticoid-Induced Leucine Zipper (GILZ) in Inflammatory Bone Loss. *PLoS ONE* **2017**, *12*, e0181133, doi:10.1371/journal.pone.0181133.
41. Fan, H.; Kao, W.; Yang, Y.H.; Gu, R.; Harris, J.; Fingerle-Rowson, G.; Bucala, R.; Ngo, D.; Beaulieu, E.; Morand, E.F. Macrophage Migration Inhibitory Factor Inhibits the Antiinflammatory Effects of Glucocorticoids via Glucocorticoid-Induced Leucine Zipper. *Arthritis Rheumatol* **2014**, *66*, 2059–2070, doi:10.1002/art.38689.
42. Agarwal, S.; Mirzoeva, S.; Readhead, B.; Dudley, J.T.; Budunova, I. PI3K Inhibitors Protect against Glucocorticoid-Induced Skin Atrophy. *EBioMedicine* **2019**, *41*, 526–537, doi:10.1016/j.ebiom.2019.01.055.
43. Carruthers, C.W.; Suh, J.H.; Gustafsson, J.-A.; Webb, P. Phosphorylation of Glucocorticoid Receptor Tau1c Transactivation Domain Enhances Binding to CREB Binding Protein (CBP) TAZ2. *Biochemical and Biophysical Research Communications* **2015**, *457*, 119–123, doi:10.1016/j.bbrc.2014.12.021.
44. Tonsing-Carter, E.; Hernandez, K.M.; Kim, C.R.; Harkless, R.V.; Oh, A.; Bowie, K.R.; West-Szymanski, D.C.; Betancourt-Ponce, M.A.; Green, B.D.; Lastra, R.R.; et al. Glucocorticoid Receptor Modulation Decreases ER-Positive Breast Cancer Cell Proliferation and Suppresses Wild-Type and Mutant ER Chromatin Association. *Breast Cancer Res* **2019**, *21*, 82, doi:10.1186/s13058-019-1164-6.
45. Cai, L.; Hua, C.; Geng, Y.; Chen, Q.; Niu, L.; Tao, S.; Ni, Y.; Zhao, R. Chronic Dexamethasone Exposure Activates the TLR4-Mediated Inflammation Pathway and Induces Epithelial Apoptosis in the Goat Colon. *Biochem Biophys Res Commun* **2019**, *518*, 7–13, doi:10.1016/j.bbrc.2019.07.071.
46. Cacheiro-Llaguno, C.; Hernández-Subirá, E.; Díaz-Muñoz, M.D.; Fresno, M.; Serrador, J.M.; Íñiguez, M.A. Regulation of Cyclooxygenase-2 Expression in Human T Cells by Glucocorticoid Receptor-Mediated Transrepression of Nuclear Factor of Activated T Cells. *IJMS* **2022**, *23*, 13275, doi:10.3390/ijms232113275.
47. Lesovaya, E.A.; Savinkova, A.V.; Morozova, O.V.; Lylova, E.S.; Zhidkova, E.M.; Kulikov, E.P.; Kirsanov, K.I.; Klopot, A.; Baida, G.; Yakubovskaya, M.G.; et al. A Novel Approach to Safer Glucocorticoid Receptor-Targeted Anti-Lymphoma Therapy via REDD1 (Regulated in Development and DNA Damage 1) Inhibition. *Mol Cancer Ther* **2020**, *19*, 1898–1908, doi:10.1158/1535-7163.MCT-19-1111.
48. Shimizu, N.; Yoshikawa, N.; Ito, N.; Maruyama, T.; Suzuki, Y.; Takeda, S.; Nakae, J.; Tagata, Y.; Nishitani, S.; Takehana, K.; et al. Crosstalk between Glucocorticoid Receptor and Nutritional Sensor mTOR in Skeletal Muscle. *Cell Metabolism* **2011**, *13*, 170–182, doi:10.1016/j.cmet.2011.01.001.
49. Frenkel, B.; White, W.; Tuckermann, J. Glucocorticoid-Induced Osteoporosis. In *Glucocorticoid Signaling*; Wang, J.-C., Harris, C., Eds.; Advances in Experimental Medicine and Biology; Springer New York: New York, NY, 2015; Vol. 872, pp. 179–215 ISBN 978-1-4939-2894-1.
50. Dodonova, S.A.; Zhidkova, E.M.; Kryukov, A.A.; Valiev, T.T.; Kulikov, E.P.; Yakubovskaya, M.G.; Lesovaya, E.A. Side Effects of Glucocorticoids: In Vivo Models and Underlying Mechanisms. *Discov Med* **2025**, *2*, 212, doi:10.1007/s44337-025-00453-z.
51. Wu, T.; Wang, F.; Ai, C.; Li, L.; Wu, F. Tangeretin Suppresses RANKL-Induced Osteoclastogenesis and Alleviates Postmenopausal Osteoporosis by Inhibiting Notch Signaling. *Regenerative Therapy* **2025**, *30*, 136–143, doi:10.1016/j.reth.2025.04.019.
52. Zhu, G.; Chen, W.; Tang, C.-Y.; McVicar, A.; Edwards, D.; Wang, J.; McConnell, M.; Yang, S.; Li, Y.; Chang, Z.; et al. Knockout and Double Knockout of Cathepsin K and Mmp9 Reveals a Novel Function of Cathepsin

 doi:10.20944/preprints202510.1879.v1



K as a Regulator of Osteoclast Gene Expression and Bone Homeostasis. *Int. J. Biol. Sci.* **2022**, *18*, 5522–5538, doi:10.7150/ijbs.72211.

53. Xiong, K.; Li, J.; Liu, Y.; Pan, Y.; Huang, Y.; Zhan, D.; Zhang, L.; Tang, M.; Li, J.; Sun, H. Lacticaseibacillus Rhamnosus LGG Suppresses Osteoclastogenesis via TLR6/NF-κB Modulation and Attenuates Ovariectomy-Induced Bone Loss in Mice. *Probiotics & Antimicro. Prot.* **2025**, doi:10.1007/s12602-025-10783-0.
54. Salemdawod, A.; Cooper, B.; Liang, Y.; Walczak, P.; Vatter, H.; Maciaczyk, J.; Janowski, M. CRISPR-Cas9 Single Nucleotide Editing of Tuberous Sclerosis Complex 2 Gene in Mesenchymal Stem Cells. *The CRISPR Journal* **2025**, 25731599251367059, doi:10.1177/25731599251367059.
55. Komori, T. Regulation of Skeletal Development and Maintenance by Runx2 and Sp7. *IJMS* **2024**, *25*, 10102, doi:10.3390/ijms251810102.
56. Huang, Y.; Seitz, D.; Chevalier, Y.; Müller, P.E.; Jansson, V.; Klar, R.M. Synergistic Interaction of hTGF-B3 with hBMP-6 Promotes Articular Cartilage Formation in Chitosan Scaffolds with hADSCs: Implications for Regenerative Medicine. *BMC Biotechnol* **2020**, *20*, 48, doi:10.1186/s12896-020-00641-y.
57. Hua, G.; Ganti, K.P.; Chambon, P. Glucocorticoid-Induced Tethered Transrepression Requires SUMOylation of GR and Formation of a SUMO-SMRT/NCoR1-HDAC3 Repressing Complex. *Proc Natl Acad Sci U S A* **2016**, *113*, E635-643, doi:10.1073/pnas.1522826113.
58. Baiula, M.; Bedini, A.; Baldi, J.; Cavet, M.E.; Govoni, P.; Spampinato, S. Mapracorat, a Selective Glucocorticoid Receptor Agonist, Causes Apoptosis of Eosinophils Infiltrating the Conjunctiva in Late-Phase Experimental Ocular Allergy. *Drug Des Devel Ther* **2014**, *8*, 745–757, doi:10.2147/DDDT.S62659.
59. De Bosscher, K.; Berghe, W.V.; Beck, I.M.E.; Van Molle, W.; Hennuyer, N.; Hapgood, J.; Libert, C.; Staels, B.; Louw, A.; Haegeman, G. A Fully Dissociated Compound of Plant Origin for Inflammatory Gene Repression. *Proc. Natl. Acad. Sci. U.S.A.* **2005**, *102*, 15827–15832, doi:10.1073/pnas.0505554102.
60. Hua, G.; Zein, N.; Daubeuf, F.; Chambon, P. Glucocorticoid Receptor Modulators CpdX and CpdX-D3 Exhibit the Same in Vivo Antiinflammatory Activities as Synthetic Glucocorticoids. *Proc Natl Acad Sci U S A* **2019**, *116*, 14191–14199, doi:10.1073/pnas.1908258116.
61. Hua, G.; Zein, N.; Paulen, L.; Chambon, P. The Glucocorticoid Receptor Agonistic Modulators CpdX and CpdX-D3 Do Not Generate the Debilitating Effects of Synthetic Glucocorticoids. *Proc Natl Acad Sci U S A* **2019**, *116*, 14200–14209, doi:10.1073/pnas.1908264116.
62. Coghlan, M.J.; Jacobson, P.B.; Lane, B.; Nakane, M.; Lin, C.W.; Elmore, S.W.; Kym, P.R.; Luly, J.R.; Carter, G.W.; Turner, R.; et al. A Novel Antiinflammatory Maintains Glucocorticoid Efficacy with Reduced Side Effects. *Mol Endocrinol* **2003**, *17*, 860–869, doi:10.1210/me.2002-0355.
63. van Lierop, M.-J.C.; Alkema, W.; Laskewitz, A.J.; Dijkema, R.; van der Maaden, H.M.; Smit, M.J.; Plate, R.; Conti, P.G.M.; Jans, C.G.J.M.; Timmers, C.M.; et al. Org 214007-0: A Novel Non-Steroidal Selective Glucocorticoid Receptor Modulator with Full Anti-Inflammatory Properties and Improved Therapeutic Index. *PLoS One* **2012**, *7*, e48385, doi:10.1371/journal.pone.0048385.
64. De Bosscher, K.; Beck, I.M.; Haegeman, G. Classic Glucocorticoids versus Non-Steroidal Glucocorticoid Receptor Modulators: Survival of the Fittest Regulator of the Immune System? *Brain, Behavior, and Immunity* **2010**, *24*, 1035–1042, doi:10.1016/j.bbi.2010.06.010.
65. Karra, A.G.; Tziortziou, M.; Kylindri, P.; Georgatza, D.; Gorgogietas, V.A.; Makiou, A.; Krokida, A.; Tsialtas, I.; Kalousi, F.D.; Papadopoulos, G.E.; et al. Boswellic Acids and Their Derivatives as Potent Regulators of Glucocorticoid Receptor Actions. *Archives of Biochemistry and Biophysics* **2020**, *695*, 108656, doi:10.1016/j.abb.2020.108656.
66. Leão, T.K.; Ribeiro, D.L.; Machado, A.R.T.; Costa, T.R.; Sampaio, S.V.; Antunes, L.M.G. Synephrine and Caffeine Combination Promotes Cytotoxicity, DNA Damage and Transcriptional Modulation of Apoptosis-Related Genes in Human HepG2 Cells. *Mutation Research/Genetic Toxicology and Environmental Mutagenesis* **2021**, *868–869*, 503375, doi:10.1016/j.mrgentox.2021.503375.
67. Ribeiro, D.L.; Machado, A.R.T.; Da Silva Machado, C.; Santos, P.W.D.S.; Aissa, A.F.; Barcelos, G.R.M.; Antunes, L.M.G. Analysis of the Cytotoxic, Genotoxic, Mutagenic, and pro-Oxidant Effect of Synephrine, a Component of Thermogenic Supplements, in Human Hepatic Cells in Vitro. *Toxicology* **2019**, *422*, 25–34, doi:10.1016/j.tox.2019.04.010.

 doi:10.20944/preprints202510.1879.v1



68. Ribeiro, D.L.; Machado, A.R.T.; Machado, C.; Ferro Aissa, A.; Dos Santos, P.W.; Barcelos, G.R.M.; Antunes, L.M.G. *P* -Synephrine Induces Transcriptional Changes via the cAMP/PKA Pathway but Not Cytotoxicity or Mutagenicity in Human Gastrointestinal Cells. *Journal of Toxicology and Environmental Health, Part A* **2021**, *84*, 196–212, doi:10.1080/15287394.2020.1855490.
69. Li, L.; Lou, Z.; Wang, L. The Role of FKBP5 in Cancer Aetiology and Chemoresistance. *Br J Cancer* **2011**, *104*, 19–23, doi:10.1038/sj.bjc.6606014.
70. Pei, H.; Li, L.; Fridley, B.L.; Jenkins, G.D.; Kalari, K.R.; Lingle, W.; Petersen, G.; Lou, Z.; Wang, L. FKBP51 Affects Cancer Cell Response to Chemotherapy by Negatively Regulating Akt. *Cancer Cell* **2009**, *16*, 259–266, doi:10.1016/j.ccr.2009.07.016.